

# Zeno Behavior in Electromechanical Hybrid Systems: From Theory to Experimental Validation

Shishir Nadubettu Yadukumar, Bhargav Kothapalli and Aaron D. Ames

**Abstract**—The goal of this paper is to assess the capacity of Zeno phenomena to correctly predict the behavior of real physical systems. We begin by considering electromechanical hybrid systems. Formal conditions are given on when systems of this form display Zeno behavior, in which case the hybrid model is *completed* to allow for solutions to be carried past the Zeno point. The end result is periods of unconstrained and constrained motion, with transitions to the constrained motion occurring at the *Zeno point*, i.e., a *Zeno periodic orbit*. We then consider a double pendulum with a mechanical stop controlled by a DC motor, use these formal methods to predict the existence of a Zeno periodic orbit in simulation, and verify through experimentation that Zeno behavior provides an accurate description of the behavior of the physical system.

## I. INTRODUCTION

Hybrid dynamical systems are systems that display both continuous and discrete behavior [8], [15], [24]. As such, they describe a large class of physical systems, especially those undergoing impacts. A fundamental phenomenon which is unique to hybrid systems is Zeno behavior, where an infinite number of discrete transitions occur in a finite amount of time. Since its introduction, Zeno behavior has been well studied due to the way in which it prevents the extension of standard notions of solutions to the hybrid framework; Zeno solutions, by definition, only exist for a finite period of time.

Zeno behavior has been well studied in the hybrid systems community for ten years now [2], [6], [7], [9], [10], [11], [26], yet the hybrid systems community still remains divided over its existence in the real world. One side of the discussion claims that since it occurs as a result of instantaneous discrete changes in a system, which cannot occur in reality, Zeno behavior itself does not occur in reality. As a result, Zeno behavior is thus not interesting, and instead the model of the system being studied should be refined so that Zeno behavior does not occur. The other side of the discussion claims that although Zeno behavior does not occur in reality, modeling of systems with instantaneous discrete changes is “close” to reality, and therefore system models with Zeno behavior will display behavior that is “close” to the physical behavior—it is therefore important to study Zeno behavior. The authors, admittedly, come from the latter camp and have established numerous formal results related to Zeno behavior. Specifically, results that relate Zeno behavior to a type of equilibria unique to hybrid systems, termed *Zeno*

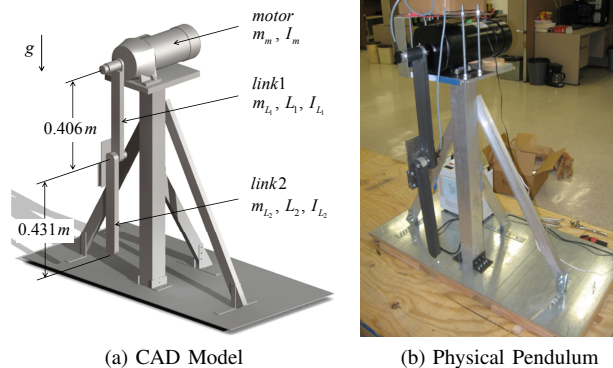


Fig. 1: Double pendulum with a mechanical stop.

*equilibria*, and the existence of Zeno behavior to the stability of these equilibria (see [12], [14], [19], [21]). This allowed for conditions for the existence of Zeno behavior, and for hybrid models to be *completed* so that Zeno solutions can be extended beyond their finite limit points.

The goal of this paper is to present a physical grounding for the formal ideas that have been considered relating to Zeno behavior. Specifically, this paper studies existence of Zeno behavior in electromechanical hybrid systems, giving conditions for the existence of Zeno behavior and verifying these conditions through experimentation. To achieve these results, we begin by considering a special class of hybrid electromechanical systems modeling mechanical systems undergoing impacts and driven by DC motors. Formal conditions for the existence of Zeno behavior in systems of this form are given, and these conditions are used to *complete* the hybrid system model to allow for solutions to be carried past the Zeno point—this results in periods of unconstrained and constrained motion, with transitions to the constrained motion occurring at the *Zeno point*. Utilizing this formal theory, we consider a double pendulum with a mechanical stop where the top link is driven by a permanent magnet DC motor and demonstrate that, due to the mechanical stop, the electromechanical hybrid model for this system displays Zeno behavior. As a result, this model is completed and, through simulation, we find a periodic orbit in this completed system, i.e., a *Zeno periodic orbit*. We then verify, through experimentation, that the formal methods provide an accurate description of the behavior of the physical system—the Zeno periodic orbit found through simulation occurs on the physical system.

This work is supported by NSF grant CNS-0953823.

S. Nadubettu Yadukumar is with the Department of Electrical Engineering, B. Kothapalli graduated from the department of Mechanical Engineering and A. D. Ames is with the Faculty of Mechanical Engineering, Texas A&M University, College Station, Texas, USA {shishirny, bhargav.1985, aames}@tamu.edu

## II. ELECTROMECHANICAL HYBRID SYSTEMS

In this section, we introduce the *extended Lagrangian* system and eventually the associated extended Lagrangian hybrid system. This section will also discuss the presence of *holonomic* and *unilateral* constraints that will be important due to the mechanical stop. Hybrid systems of this form have been studied in the context of *Lagrangian hybrid* systems in Zeno behavior, see [2], [3], [13], and were also formulated as linear complementarity systems in [16] and [22].

**Dynamical systems:** Let  $q \in Q$  be the *configuration space* of a mechanical system.<sup>1</sup> We will consider the Lagrangian,  $L : TQ \rightarrow \mathbb{R}$ , describing mechanical or robotic systems:

$$L(q, \dot{q}) = \frac{1}{2} \dot{q}^T M(q) \dot{q} - V(q), \quad (1)$$

yielding  $M(q)\ddot{q} + C(q, \dot{q})\dot{q} + N(q) = \Upsilon$ , with  $\Upsilon$  being the control input.

For an electrical system, the generalized coordinates are chosen as inductor currents,  $i_M^T = [i_1, i_2, \dots, i_{n_M}]$ , and capacitor voltages,  $v_E^T = [v_1, v_2, \dots, v_{n_E}]$ . Therefore, when an electrical system is included with a mechanical system (*called the electromechanical system*), we obtain the *Extended Lagrangian*,  $L_e : TQ_e \rightarrow \mathbb{R}$ , and is given by:

$$L_e(q, \dot{q}, i_M, v_E) = L(q, \dot{q}) + W_e(i_M, v_E, q), \quad (2)$$

where  $W_e(i_M, v_E, q)$  is the energy stored in the magnetic and electric fields of the system.

In this paper, we will consider a particular case of electromechanical system which comprises of  $n_M$  permanent magnet DC (PMDC) drives (since most of the electromechanical systems have motors as primary actuators, including the system considered in this paper). In this case  $W_e$  becomes:

$$W_e(i_M, q) = \frac{1}{2} i_M^T \mathcal{L}_M i_M - K_\omega \cos(q) i_M. \quad (3)$$

A detailed derivation of this realization can be found in [25].  $\mathcal{L}_M \in \mathbb{R}^M \times \mathbb{R}^M$  is the inductance matrix<sup>2</sup> and  $K_\omega \in \mathbb{R}^M \times \mathbb{R}^M$  is the diagonal matrix of motor constants of the motors. The resulting motor dynamics is given by:

$$\mathcal{R}_M i_M + \mathcal{L}_M \dot{i}_M + K_\omega \dot{q} = \mathcal{V}_M(q, \dot{q}), \quad (4)$$

where  $\mathcal{R}_M \in \mathbb{R}^M \times \mathbb{R}^M$  is the resistance matrix,  $\mathcal{V}_M \in \mathbb{R}^M$ , a function of position and velocity of the mechanical system, is the feedback control law input in the form of voltage. Also, the torque  $\Upsilon$ , will be a function of current  $\Upsilon(i_M) = K_\phi i_M$ , where  $K_\phi \in \mathbb{R}^M \times \mathbb{R}^M$  is the diagonal matrix of torque constants of the motors.

Defining the *state* of the system as  $x = (q, \dot{q}, i_M)$ , the vector field,  $f_{L_e}$  associated with the extended Lagrangian  $L_e$  of the form (2), takes the following form:

$$\begin{aligned} \dot{x} &= f_{L_e}(x) \\ &= \begin{pmatrix} \dot{q} \\ M(q)^{-1} (-C(q, \dot{q})\dot{q} - N(q) + K_\phi i_M) \\ \mathcal{L}_M^{-1} (\mathcal{V}_M(q, \dot{q}) - \mathcal{R}_M i_M - K_\omega \dot{q}) \end{pmatrix}. \end{aligned} \quad (5)$$

<sup>1</sup>For simplicity, in the models considered, we assume that the configuration space is identical to  $\mathbb{R}^n$

<sup>2</sup>having  $n_M$  DC motors is equivalent to having  $n_M$  magnetic fields

The readers should make note of the fact that the *Lagrangian* (not  $W_e(i_M, q)$ ) includes the mechanical dynamics of the rotors and gearboxes.

**Holonomic constraints:** The constraints that we consider in this paper are only mechanical constraints and not electrical constraints. In the presence of a constraint,  $\eta$ , for the state  $x = (q, \dot{q}, i_M)$ , we have (see [18]):

$$\dot{x} = f_{L_e}^\eta(x) = f_{L_e}(x) + \begin{pmatrix} 0 \\ M(q)^{-1} d\eta(q)^T \lambda(q, \dot{q}) \\ 0 \end{pmatrix}. \quad (6)$$

Here  $\lambda$  is the Lagrange multiplier which represents the contact force and  $d\eta(q) = \left(\frac{\partial \eta}{\partial q}(q)\right)^T$ .

**Unilateral Constraints:** The domain, guard and reset map (or impact equations) will be obtained from *unilateral constraint*  $h : Q_e \rightarrow \mathbb{R}$  which gives the set of admissible configurations of the system; we assume that the zero level set  $h^{-1}(0)$  is a smooth manifold.

Define the domain and guard, respectively, as

$$\begin{aligned} D_h &= \{(q, \dot{q}, i_M) \in TQ : h(q) \geq 0\}, \\ G_h &= \{(q, \dot{q}, i_M) \in TQ : h(q) = 0 \text{ and } dh(q)\dot{q} \leq 0\}. \end{aligned} \quad (7)$$

The reset map associated to a unilateral constraint is obtained through impact equations of the form (see [5], [17]):

$$R_h(q, \dot{q}, i_M) = \begin{pmatrix} q \\ \dot{q} - (1 + \varepsilon) \frac{dh(q)\dot{q}}{dh(q)M(q)^{-1}dh(q)^T} M(q)^{-1} dh(q)^T \\ i_M \end{pmatrix} \quad (8)$$

Here  $0 \leq \varepsilon \leq 1$  is the *coefficient of restitution*. This reset map corresponds to rigid-body collision under the assumption of *frictionless impact*, [5] and [23].

**Definition 1:** A *simple electromechanical hybrid Lagrangian* (or *hybrid extended Lagrangian*) is defined to be a tuple  $\mathbf{L}_e = (Q_e, L_e, h)$ , where  $Q_e$  is the *configuration space* (assumed to be<sup>3</sup>  $\mathbb{R}^{n+n_M+n_E}$ ),  $L_e : TQ_e \rightarrow \mathbb{R}$  is an *extended Lagrangian* of the form (2),  $h : Q_e \rightarrow \mathbb{R}$  is a *unilateral constraint*. Given a hybrid extended Lagrangian  $\mathbf{L}_e = (Q_e, L_e, h)$ , associated is the simple electromechanical hybrid system (SEHS):

$$\mathcal{S}\mathcal{H}_{L_e} = (D_h, G_h, R_h, f_{L_e}).$$

If the electromechanical system were to be eliminated from the Hybrid system, then  $\mathcal{S}\mathcal{H}_{L_e}$  becomes a *Lagrangian Hybrid system* consisting of only the dynamics of Lagrangian systems.

## III. ZENO BEHAVIOR

We now introduce Zeno behavior and the corresponding notion of Zeno equilibria, and we consider the stability of these equilibria. Note that space constraints prevent the introduction of the definition of executions [21] but, intuitively speaking, an execution  $\chi = (\Lambda, \mathcal{I}, \mathcal{C})$ , where  $\Lambda \subseteq \mathbb{N}$  is an

<sup>3</sup>Again, for  $n_L$  DC motors alone,  $n_C = 0$ , implying  $Q_e \in \mathbb{R}^{n+n_M}$

indexing set,  $\mathcal{I} = \{I_i\}_{i \in \Lambda}$  is a collection of intervals, e.g.,  $I_i = [t_i, t_{i+1}]$ , and  $\mathcal{C} = \{c_i\}_{i \in \Lambda}$  is a set of *trajectories*, i.e., they must satisfy  $\dot{c}_i(t) = f_{L_e}(c_i(t))$  on  $I_i$  along with some “consistency” conditions:  $c_i(t_{i+1}) \in G_h$  and  $R_h(c_i(t_{i+1})) = c_{i+1}(t_{i+1})$ . An execution  $\chi$  is *Zeno* if  $\Lambda = \mathbb{N}$  and

$$t_\infty := \lim_{k \rightarrow \infty} t_k - t_0 = \sum_{k=0}^{\infty} t_{k+1} - t_k < \infty.$$

Here  $t_\infty$  is called the *Zeno time*. If  $\chi$  is a Zeno execution of a SEHS,  $\mathcal{S}\mathcal{H}_{L_e}$ , then its *Zeno point* is defined to be

$$x_\infty = (q_\infty, \dot{q}_\infty, t_{M_\infty}) = \lim_{k \rightarrow \infty} c_k(t_k) = \lim_{k \rightarrow \infty} (q_k(t_k), \dot{q}_k(t_k), t_{M_k}(t_k)).$$

These limit points are intricately related to a type of equilibrium point that is unique to hybrid systems: Zeno equilibria.

**Definition 2:** A *Zeno equilibrium point* of a SHS  $\mathcal{S}\mathcal{H}$  is a point  $x^* \in G$  such that  $R(x^*) = x^*$  and  $f(x^*) \neq 0$ .

The following theorem, which is a straightforward extension of the results of [12], [13], [14] to simple electromechanical hybrid systems, provides sufficient conditions for existence of Zeno executions in the vicinity of a Zeno equilibrium point.

**Theorem 1:** Let  $\mathcal{S}\mathcal{H}_{L_e}$  be a simple electromechanical Lagrangian hybrid system and let  $x^* = (q^*, \dot{q}^*, t_M^*)$  be a Zeno equilibrium point of  $\mathcal{S}\mathcal{H}_{L_e}$ . If  $0 \leq \varepsilon < 1$  and  $\dot{h}(q^*, \dot{q}^*, t_M^*) < 0$ , there exists a neighborhood  $\mathcal{W} \subset D_{L_e}$  of  $(q^*, \dot{q}^*, t_M^*)$  such that for every  $(q_0, \dot{q}_0, t_{M_0}) \in \mathcal{W}$ , there is unique Zeno execution  $\chi$  of  $\mathcal{S}\mathcal{H}_{L_e}$  with  $c_0(\tau_0) = (q_0, \dot{q}_0, t_{M_0})$ .

This theorem is essential to this paper because, if a system is determined to be Zeno through these conditions, it is necessary to *complete* this system to allow solutions to be carried past Zeno points.

**Completed Hybrid Systems:** A completed hybrid system consists of hybrid dynamics and constrained dynamics, with transitions between these two types of dynamics (see Fig. 2 for a graphical representation of a completed hybrid system). The idea is that, if the system has stable Zeno equilibria it evolves according to the hybrid dynamics until the Zeno point is reached, at which time a transition to the constrained dynamics is made. Formally, completed hybrid systems have been defined in the following manner (see [3], [4], [16], [19], [20], [21]):

$$\overline{\mathcal{S}\mathcal{H}_{L_e}} = \begin{cases} \mathcal{D}_h & \text{if } h(q) = 0, dh(q)\dot{q} = 0, \\ & \text{and } \lambda(q, \dot{q}) > 0 \\ \mathcal{S}\mathcal{H}_{L_e} & \text{otherwise} \end{cases}$$

where  $\mathcal{D}_h$  is the dynamical system on the surface  $h = 0$  obtained by enforcing the holonomic constraint  $h$ .

We can consider solutions to completed hybrid systems by concatenating solutions to its individual components. Intuitively, a solution to a completed hybrid system consists of unconstrained motion, followed by constrained motion (when the Zeno point is reached), followed again by unconstrained motion (when the lagrange multiplier changes sign). This idea is made precise in the following definition: Given a completed system  $\overline{\mathcal{S}\mathcal{H}_{L_e}}$ , a completed execution is  $\bar{\chi}$  of

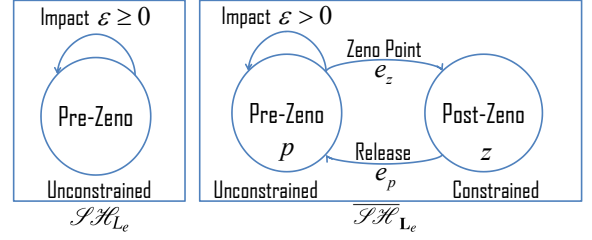


Fig. 2: A graphical representation of a SEHS and its associated completed hybrid system.

$\overline{\mathcal{S}\mathcal{H}_{L_e}}$  is a sequence of alternating hybrid and constrained executions of  $\bar{\chi} = \{\chi^{(1)}, \tilde{\chi}^{(2)}, \chi^{(3)}, \tilde{\chi}^{(4)}, \dots\}$  that satisfies the following conditions:

- (i) For  $\chi^{(i)}$  and  $\tilde{\chi}^{(i+1)}$ ,  $\tau_\infty^{(i)} = \tilde{\tau}_0^{(i+1)}$  and  $c_\infty^{(i)} = \tilde{c}_0^{(i+1)}(\tilde{\tau}_0^{(i+1)})$
- (ii) For  $\tilde{\chi}^{(i)}$  and  $\chi^{(i+1)}$ ,  $\tilde{\tau}_f^{(i)} = \tau_0^{(i+1)}$  and  $\tilde{c}_f^{(i)} = c_0^{(i+1)}(\tau_0^{(i+1)})$

where the superscript  $(i)$  denotes the values corresponding to the  $i^{\text{th}}$  execution  $\chi_i$  or  $\tilde{\chi}_i$ , with  $t_\infty^{(i)}, c_\infty^{(i)}$  denoting the Zeno time and Zeno point in the case when the  $i^{\text{th}}$  execution is a Zeno execution  $\chi_i$ .

A *Zeno periodic orbit* is a completed execution  $\bar{\chi}$  with initial condition  $\tilde{c}^{(1)}(0) = x^*$  that satisfies  $c_\infty^{(2)} = \tilde{c}^{(3)}(t_0^{(3)}) = x^*$ . The period of  $\bar{\chi}$  is  $T = t_\infty^{(2)} = \tilde{t}_0^{(3)}$ . In other words, this orbit consists of a constrained execution starting at  $x^*$ , followed by a Zeno execution with infinite number of non-plastic impacts, which converges in finite time back to  $x^*$ . If  $\varepsilon = 0$ , then it is called a *simple periodic orbit*.

**Simulating completed hybrid systems.** Due to the fact that completed hybrid systems have Zeno executions, and because it is not possible to compute the entirety of these executions, a procedure must be given to simulate completed hybrid systems. Such a procedure is developed formally in [20], [21], but for the purposes of this paper, we only discuss the practical aspects of this approach. First, a hybrid execution is simulated, until it reaches an impact at some time  $t_k$ , with the state  $(q(t_k), \dot{q}(t_k), t_M)$  satisfying  $|\dot{h}(q(t_k))| < \delta$  with  $\delta > 0$  a sufficiently small simulation parameter. (This implies that the execution is “close” to the Zeno point which satisfies  $\dot{h}(q(t_k), \dot{q}(t_k), t_M(t_k)) = 0$ .) When this condition is satisfied, the hybrid execution is truncated and the algorithm applies a reinitialization map,  $(q^*, \dot{q}^*, t_M^*) = R^*(q(t_k), \dot{q}(t_k), t_M(t_k))$ , with  $R^*$  being the reset map (given in (8)) and  $\varepsilon = 0$  (i.e., it applies a perfectly plastic impact). This guarantees that  $(q^*, \dot{q}^*, t_M^*)$  is a Zeno equilibrium. At this point, the constrained dynamics (6) are simulated with  $(q^*, \dot{q}^*, t_M^*)$  as an initial condition. If it is detected that  $\lambda = 0$ , the simulation switches back to the hybrid system and the process is repeated.

#### IV. MODELING THE DOUBLE PENDULUM WITH A MECHANICAL STOP

We now consider the hybrid system model of the physical “Zeno system” that will be used: a double pendulum with a mechanical stop and with the top link being controlled by a PMDC motor (see Fig. 3). The goal of this section is

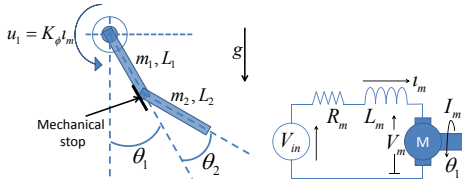


Fig. 3: A graphical representation of a double pendulum with a mechanical stop on the left and the circuit used for controlling the motor on the right.

to discuss how this system is modeled as a hybrid system, show formally that the system has Zeno behavior, use this knowledge to complete the hybrid system model and finally simulate the system. In the end we find that the simulated system has a Zeno periodic orbit. It is important to note that the analysis done in this section is much like what any researcher would do studying hybrid systems with Zeno behavior.

Consider a double pendulum with a mechanical stop (Fig. 3). This system has rigid links *link1* and *link2* of lengths  $L_1, L_2$  and masses  $m_{1L}, m_{2L}$  respectively, attached to each other through a passive joint. *Link1* is actuated by a *permanent magnet DC motor* for controlling the trajectories (see Fig. 3). In this model the masses of the first link ( $m_{1L}$ ) and the rotating parts (armature and gear box) of the motor ( $m_m$ ) are included together and denoted as  $m_1 (:= m_{1L} + m_m)$ , while the mass of the second link is denoted as  $m_2 (:= m_{2L})$ . The resulting shift in the center of mass is also included while computing the moments of inertia.

To construct the hybrid system model for the double pendulum, we begin by considering the hybrid extended Lagrangian:  $\mathbf{L}_{P_e} = (Q_{P_e}, L_{P_e}, h_{P_e})$ , where  $Q_{P_e}$  is the configuration space spanned by  $q = (\theta_1, \theta_2, t_m)$ , where  $\theta_1$  is the angle between *link1* and vertical line from top end of *link1* to ground (see Fig. 3),  $\theta_2$  is relative angle between *link1* and *link2* (constrained to be positive), and  $t_m$  is the motor current.  $L_{P_e}$  is the extended Lagrangian for the electromechanical system (given in Fig. 3), which thus has the standard form given in (2). The unilateral constraint  $h_{P_e}$  describes the constraint on *link2*, i.e., it is not allowed to pass through the mechanical stop, and is thus given by:  $h_{P_e}(q) = \theta_2$ . The state-space of the electromechanical system is given by  $(q, \dot{q}, t_m) = (\theta_1, \theta_2, \dot{\theta}_1, \dot{\theta}_2, t_m)$ . From the hybrid extended Lagrangian  $\mathbf{L}_{P_e}$  we obtain a simple hybrid system given by:

$$\mathcal{SH}_{P_e} = (D_{P_e}, G_{P_e}, R_{P_e}, f_{P_e}).$$

The domain and guard are given as in (7). In particular, the guard  $G_{P_e}$  is the subset of domain  $D_{P_e}$  where *link2* is “locked” to mechanical stop. The reset map,  $R_{P_e}(q, \dot{q}, t_m)$  is given as in (8). Finally, the vector field  $f_{P_e}$  is an extended Lagrangian vector field of the form (5) with the vector  $t_M$  having only one motor,  $t_m$ .

Torque is controlled indirectly by varying the voltage inputs to the motors. A simple P-D control law is adopted with  $\theta_1, \dot{\theta}_1$  being the inputs:

$$\mathcal{V}_{in}(q, \dot{q}) = -K_p \theta_1 - K_d \dot{\theta}_1, \quad (9)$$

**Formally verifying Zeno behavior.** We now verify Theorem 1 for the double pendulum model considered. This is an important step in the simulation process, because if the model has stable Zeno equilibria it implies that it will display Zeno behavior for a non-trivial set of initial conditions. Therefore, the model must be completed to allow solutions to be taken past the Zeno points.

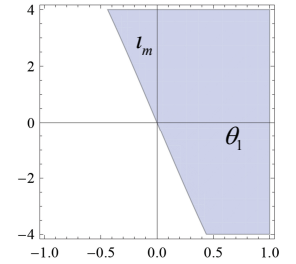
For the double pendulum, the set of Zeno equilibria is:

$$Z_P = \{(\theta_1, \theta_2, \dot{\theta}_1, \dot{\theta}_2, i_m) \in D_P : \theta_2 = 0, \dot{\theta}_2 = 0, f_{P_e} \neq 0\},$$

that is, the set of Zeno equilibria are the set of points where the lower link is “locked”. Taking the second derivative of the unilateral constraint  $h_{P_e}(q, \dot{q}, t_m)$  leads to  $\ddot{h}_{P_e}(q, \dot{q}, t_m) = \ddot{\theta}_2$ . Therefore as long as  $\ddot{\theta}_2 < 0$  immediately after every impact the system is *Zeno stable* (per Theorem 1). We thus need to find the conditions on the configuration of the system where this inequality holds. In particular  $\ddot{\theta}_2(t)$  can be obtained from the vector field (5):  $\ddot{\theta}_2(t) = (f_{P_e}(x))_{\ddot{\theta}_2}$ . Due to the complexity of the model being considered, it is not possible to simply state this expression in symbolic form. But, for the double pendulum considered for the experiment, with all the physical parameters substituted,  $\ddot{h}$  is found to be:

$$\ddot{h}_P(q, \dot{q}, i_m) = -(2.92437)i_m - (27.5697)\sin(\theta_1).$$

The blue region in the figure on the right indicates where  $\ddot{h} < 0$ . It can be inferred from this figure that the stable Zeno equilibria are essentially the set of Zeno equilibria where  $\theta_1$  is positive, i.e., where the pendulum is swinging “to the right.” This is a large set of configurations, so the double pendulum with a mechanical stop is Zeno and it is necessary to complete this hybrid system.



Since we will have *stable Zeno equilibria* at a large collection of points, the system can be taken past the *Zeno point*, which basically means that the double pendulum will “lock” after *Zeno* execution. That is, we obtain a vector field,  $f_{P_e}^\eta$ , for the constrained system (in better terms “locked system”), which is given as in (6) with  $\eta = h_{P_e}$ . Thus, the completed double pendulum system is given as in (9) by  $\overline{\mathcal{SH}}_{L_e}$ , where the  $\mathcal{D}_{h_{P_e}}$  is the “constrained” system with dynamics given by  $f_{P_e}^\eta$  corresponding to the pendulum being “locked” and  $\mathcal{SH}_{L_e}$  is the “unconstrained system” corresponding to the pendulum being in “unlocked” position. We can thus simulate this resulting complete hybrid system through the methods discussed in Section III.

**Simulating the Double Pendulum Model.** Fig. 1(a) shows a CAD model of the double pendulum considered for the experiment. Even with the data sheets, it was not possible to estimate all of these values accurately due to missing data. For example, the inertia of the motor specified in the datasheet was without the gearbox included, and the resistance specified was only for the motor winding. Thus

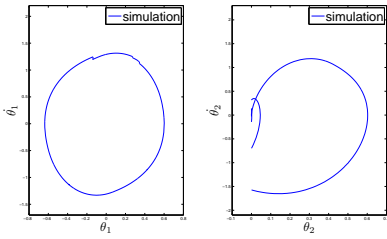


Fig. 4: Simulation results: phase portrait of  $(\theta_1, \dot{\theta}_1)$  (left) and  $(\theta_2, \dot{\theta}_2)$  (right) for the completed hybrid system modeling the double pendulum with a mechanical stop.

the estimated parameters had to be “tuned” to better reflect the physical properties of the system that it was not possible to estimate. For example, the resistance of the circuit, which have MOSFETs (Metal Oxide Semi-conductor Field Effect Transistor) for switching the H-bridge, must be taken into account when determining the parameters of the system. As a result, and coupled with a detailed Solidworks model (Fig. 1(a)), we are able to determine the physical parameters of the system used in simulation, to accurately represent the physical parameters of the system shown in Fig. 1.

From the estimated physical parameters for the system, we are able to simulate the double pendulum. Since the goal is to validate Zeno behavior as a modeling paradigm, we looked for control gains that resulted in a Zeno periodic orbit in the completed hybrid system. In particular, we found that for  $K_p = 2.5$  and  $K_d = -1$  the end result is a Zeno periodic orbit, which can be seen in Fig. 4 which shows the phase portraits for this orbit. The top of the  $(\theta_1, \dot{\theta}_1)$  phase portrait shows jumps due to the presence of impacts of *link2* with *link1*. Same is true with the second phase portrait,  $(\theta_2, \dot{\theta}_2)$ , with jumps being seen when  $\theta_2 = 0$ . Since the impacts are lossy,  $\dot{\theta}_2$  changes from negative to positive and with a smaller magnitude. Eventually, the solution reaches the *Zeno* point and then the pendulum resumes normal *constrained* motion. This cycle repeats with alternating phases of constrained and unconstrained motions, indicating that it is a *Zeno periodic orbit*. The goal is to show that this simulated behavior correctly predicts the behavior of the physical system.

## V. EXPERIMENTAL RESULTS

This section discusses an experiment conducted on a double pendulum with a mechanical stop as shown in Fig. 1. The goal is to run this physical system with the same controllers as those that were established in the previous section to show that, in fact, the simulation of this system captures its physical behavior (especially with respect to Zeno behavior, completion, and the existence of a Zeno periodic orbit).

A ball, with a coefficient of restitution  $\varepsilon = 0.2$ , is placed at the mechanical stop; which includes both the energy lost in the ball and the gear train impacts. The system is then run with the same PD gains as the simulated system. The end result is a very close agreement with the simulated behavior of the system as can be seen in Fig. 5, indicating that

Zeno behavior provides a valid approximation of physical phenomena. Link to the video comparing real and simulated behavior is given in [1]. Of special interest is the fact that simulation predicted the existence of a Zeno periodic orbit, and we find that the physical system in fact displays a Zeno periodic orbit (or a physical approximation thereof). To better understand this comparison between real and simulated behavior, we discuss the plots in Fig. 5.

Fig. 5(a) shows a comparison of simulated and physical behaviors over time with the periods of constrained and unconstrained motions indicated. In the lower waveform, when  $\theta_2 > 0$  the system evolves according to the hybrid system  $\mathcal{S}\mathcal{H}\mathcal{P}_e$  until the Zeno point is reached, i.e.,  $\theta_2 = 0$ , or *link1* is “locked” to *link2*. At this point, the system evolves under the constrained dynamics, until the Lagrange multiplier changes sign and *link2* is released. Fig. 5(b) zooms into one period of the Zeno periodic orbit consisting of a Zeno solution, followed by a constrained phase, followed by release; the simulated and physical behavior are compared in this figure. One can see that there is very good agreement between the predicted and actual behavior. In particular, the simulation accurately models the first large impact in the system, and the constrained period in simulation approximates small oscillations in the physical system as a result of vibrations in the ball when *link2* is in contact with *link1*.

The phase portraits of the simulated and physical system are compared in Fig. 5(c); again, the simulated system has a Zeno periodic orbit and we find that the physical system also displays a “Zeno periodic orbit” in the sense that the phase portrait is periodic with phases of constrained and unconstrained motion, with transitions to the constrained phase occurring at the Zeno point and transitions to the unconstrained phases occurring when the *link2* is released. Note that the largest deviations for the physical and simulated system don’t occur near the impacts and Zeno points, but are rather due to time delays in the change of motor direction at the apex of the pendulum motion; a delay that the simulated system was not able to completely capture. The behavior of the simulated vs. the physical system near the Zeno point can be seen in Fig. 5(d). Here one can see very good agreement between the the predicted and actual behavior. The physical system clearly has an accumulation point in the set of Zeno equilibria just as the theory predicted.

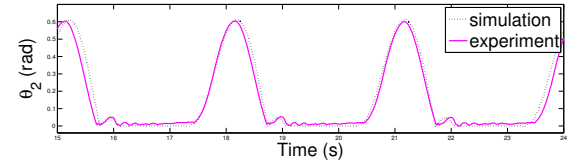
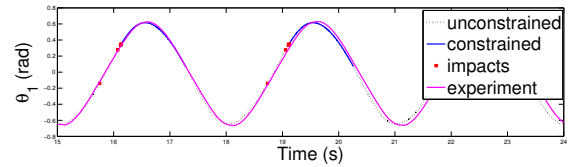
## VI. CONCLUSION

This paper showed that Zeno behavior, while it may not “exist” in reality, provides an accurate model of real physical phenomena. Moreover, all of the theory that has been proven over the years with respect to Zeno behavior is practically useful in predicting the behavior of physical systems. In particular, we utilized the notions of extended Lagrangians, Zeno equilibria, hybrid system completion, and Zeno periodic orbits. The existence of these theoretical constructs were used to properly simulate the Zeno system modeling a double pendulum with a mechanical stop. A physical version of this system was built, and the same controller applied to the simulated system was applied to this physical

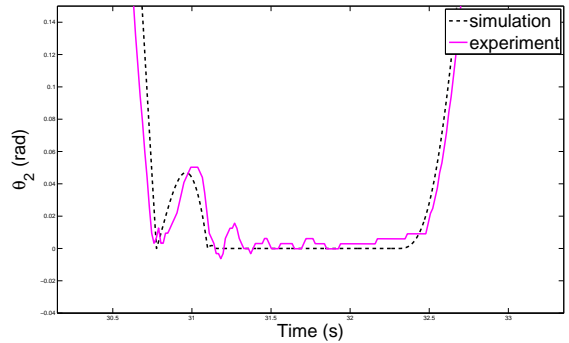
system. The end result was very good agreement between the simulated and physical behavior. This provides evidence for the claim that Zeno behavior provides a good approximation to phenomena that can occur in physical systems. As such, studying this behavior is an important research direction.

#### REFERENCES

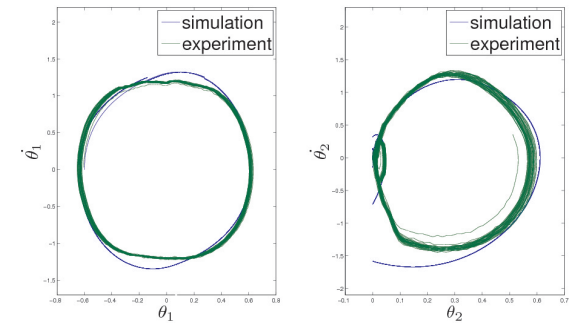
- [1] Comparison of real and simulated Zeno behavior in double pendulum. <http://www.youtube.com/watch?v=Lbqaonv7MpM>.
- [2] A. D. Ames, A. Abate, and S. Sastry. Sufficient conditions for the existence of Zeno behavior. In *44th IEEE Conference on Decision and Control and European Control Conference*, Seville, Spain, 2005.
- [3] A. D. Ames, H. Zheng, R. D. Gregg, and S. Sastry. Is there life after Zeno? Taking executions past the breaking (Zeno) point. In *Proc. American Control Conference*, pages 2652 – 2657, 2006.
- [4] J. M. Bourgeot and B. Brogliato. Asymptotic tracking of periodic trajectories for a simple mechanical systems subject to nonsmooth impacts. *IEEE Transactions on Automatic Control*, 46:1122–1126, 2001.
- [5] B. Brogliato. *Nonsmooth Mechanics*. Springer-Verlag, 1999.
- [6] R. Goebel and A. R. Teel. Lyapunov characterization of Zeno behavior in hybrid systems. In *IEEE Conference on Decision and Control*, 2008.
- [7] R. Goebel and A. R. Teel. Zeno behavior in homogeneous hybrid systems. In *IEEE Conference on Decision and Control*, 2008.
- [8] W. M. Haddad, V. S. Chellaboina, and S. G. Nersesov. *Impulsive and Hybrid Dynamical Systems: Stability, Dissipativity, and Control*. Princeton University Press, Princeton, NJ, 2006.
- [9] M. Heymann, F. Lin, G. Meyer, and S. Resmerita. Analysis of Zeno behaviors in a class of hybrid systems. *IEEE Trans. on Automatic Control*, 50(3):376–384, 2005.
- [10] J. L. J. Zhang, K. H. Johansson and S. Sastry. Zeno hybrid systems.
- [11] S. S. K. H. Johansson, J. Lygeros and M. Egerstedt. Simulation of zeno hybrid automata. In *Proceedings of the 38th IEEE Conference on Decision and Control*, Phoenix, AZ, 1999.
- [12] A. Lamperski and A. D. Ames. On the existence of Zeno behavior in hybrid systems with non-isolated Zeno equilibria. In *IEEE Conference on Decision and Control*, 2008.
- [13] A. Lamperski and A. D. Ames. Sufficient conditions for Zeno behavior in Lagrangian hybrid systems. In *HSCC*, volume 4981 of *LNCS*, pages 622–625. Springer Verlag, 2008.
- [14] A. Lamperski and A. D. Ames. Lyapunov theory for Zeno stability. To appear in *IEEE Transactions on Automatic Control*, 2012.
- [15] J. Lygeros, K. H. Johansson, S. Simic, J. Zhang, and S. Sastry. Dynamical properties of hybrid automata. *IEEE Transactions on Automatic Control*, 48:2– 17, 2003.
- [16] L. Menini and A. Tornambè. Tracking control of complementary Lagrangian hybrid systems. *International Journal of Bifurcation and Chaos*, 15(6):1839–1866, 2005.
- [17] J. J. Moreau. Unilateral contact and dry friction in finite freedom dynamics. *Nonsmooth Mechanics and Applications, CISM Courses and Lectures*, 302, 1988.
- [18] R. M. Murray, Z. Li, and S. S. Sastry. *A Mathematical Introduction to Robotic Manipulation*. Taylor & Francis/CRC, 1994.
- [19] Y. Or and A. D. Ames. Existence of periodic orbits with Zeno behavior in completed Lagrangian hybrid systems. In *HSCC, LNCS*, pages 291–305. Springer-Verlag, 2009.
- [20] Y. Or and A. D. Ames. Formal and practical completion of Lagrangian hybrid systems. In *ASME/IEEE American Control Conference*, 2009.
- [21] Y. Or and A. D. Ames. Stability and completion of Zeno equilibria in Lagrangian hybrid systems. *IEEE Transactions on Automatic Control*, 56:1322–1336, 2011.
- [22] J. Shen and J.-S. Pang. Linear complementarity systems: Zeno states. *SIAM Journal on Control and Optimization*, 44(3):1040–1066, 2005.
- [23] W. J. Stronge. *Impact Mechanics*. Cambridge University Press, 2004.
- [24] A. van der Schaft and H. Schumacher. *An Introduction to Hybrid Dynamical Systems*. Lecture Notes in Control and Information Sciences 251, Springer-Verlag, 2000.
- [25] K. S. W. Haas and R. Gahleitner. Modeling of electromechanical systems, 2000.
- [26] J. Zhang, K. H. Johansson, J. Lygeros, and S. Sastry. Dynamical systems revisited: Hybrid systems with Zeno executions. In B. Krogh and N. Lynch, editors, *HSCC*, volume 1790 of *LNCS*, pages 451–464. Springer Verlag, 2000.



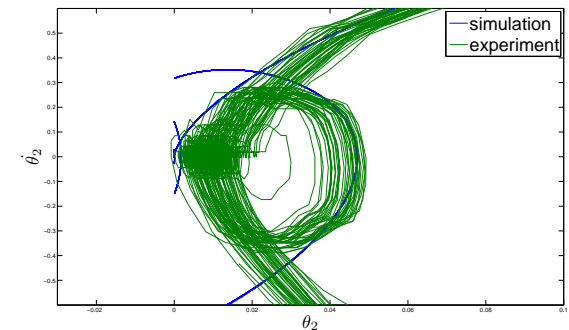
(a) The trajectories over time of both  $\theta_1$  and  $\theta_2$  with the transitions from the unconstrained dynamics indicated.



(b) A zoomed region showing the Zeno impacts following by the constrained dynamics for both the real and simulated system.



(c) The phase portraits, and hence the Zeno periodic orbits, again for the simulated and real behavior.



(d) A zoomed in region in the phase portrait near where the Zeno behavior occurs; the Zeno point is the origin of this figure.

Fig. 5: The simulated vs. physical behavior of the double pendulum with a ball with a coefficient of restitution of 0.2.